Journal of Luminescence 143 (2013) 298–303

Contents lists available at SciVerse ScienceDirect

Journal of Luminescence

journal homepage: www.elsevier.com/locate/jlumin

Down-converted luminescence and energy transfer of α-$KGd_{1-x}Eu_xF_4$ nanophosphors with selective excitation

D.K. Xu [a], S.H. Yang [a,*], Y.L. Zhang [a,b,**]

[a] State Key Laboratory of Optoelectronic Materials and Technologies, School of Physics and Engineering, Sun Yatsen University, Guangzhou 510275, PR China
[b] State Key Laboratory of Crystal Material, Shandong University, Jinan 250100, PR China

ARTICLE INFO

Article history:
Received 6 January 2013
Received in revised form
16 April 2013
Accepted 26 April 2013
Available online 7 May 2013

Keywords:
$KGd_{1-x}Eu_xF_4$
Downconversion
Dipole–dipole
Dipole–quadrupole
Lifetime

ABSTRACT

A series of $KGd_{1-x}Eu_xF_4$ (x=1, 5, 10, 15, 20, 40, 60, 80 and 100 mol%) nanophosphors were prepared by a simple and reproducible hydrothermal route. The structural and morphological properties of the samples were studied by powder X-ray diffraction (XRD) and transmission electron microscopy (TEM), showing uniform nano-sized particles with cubic phase. The excitation spectra disclosed the intrinsic absorption bands of Eu^{3+} $^5L_6$ state at 393 nm and of Gd^{3+} ^6I_J state at 272.4 nm. From the downconversion (DC) emission spectra, it was found that the optimal Eu^{3+} concentration was 20 mol% and 15 mol% under 393 nm and 272.4 nm excitation, respectively. The nonradiative energy transfer (ET) mechanism is discussed and it turns out that ET of Eu^{3+}–Eu^{3+} couple and Gd^{3+}–Eu^{3+} couple occurs mainly via electric dipole–dipole and electric dipole–quadrupole interactions, respectively. From luminescence decay curves, the lifetimes of $KGd_{1-x}Eu_xF_4$ nanophosphors are seen to decrease with the increase of Eu^{3+} concentration. Both the emission spectra and luminescence decay curves show that downconversion ET between Gd^{3+} and Eu^{3+} ions is more efficient than that between Eu^{3+} and Eu^{3+} ions, thus suggesting potential applications in mercury-free fluorescence lamp and plasma display panel under vacuum ultraviolet (VUV) radiation.

1. Introduction

Lanthanides doped nanocrystals (NCs), especially the rare-earth nanofluorides, have attracted intensive investigations for their outstanding performance such as low phonon energy, physical–chemical stability and water solubility, which lead to a wide variety of potential applications in three-dimensional displays [1], solid-state lasers [2–4], biological detection [5–7] and solar cells [8–11]. Amongst the rare-earth phosphors, the $MGdF_4$ systems ($M=Li^+$, Na^+ or K^+) are of particular interest due to their multifunctional characteristics. Firstly, as an ideal paramagnetic relaxation agent, Gd^{3+}-based compounds could be applied in magnetic resonance imaging because of its large magnetic moment and fast electronic relaxation down to nanosecond scale [5,12]. Secondly but importantly, Gd^{3+} ion can be viewed not only as a sensitizer but also as an effective sublattice-mediated energy migrator [13,14], which was precisely proved using a well-defined core–shell structure in an experimental investigation [15].

Eu^{3+} doped luminescent materials have been studied for decades due to their orange-red emission of $^5D_0\rightarrow{}^7F_J$ energy transition under VUV excitation, demonstrated by A. Meijerink's group on $LiGdF_4$:Eu^{3+} crystal, where two mechanisms, nonradiative energy transfer and cross-relaxation, might be involved in a Gd^{3+}–Eu^{3+} process by which one VUV photon results into two visible photons [16–18], which implies potential applications in color panel display and white light illumination, such as Eu^{3+} doped GdF_3 [18], $MMoO_4$ ($M=Sr^{2+}$, Ba^{2+}) [19,20], $GdAl_3(BO_3)_4$ [21], KYF_4 [22], $NaGdF_4$ [23–25], $NaGd(PO_4)_2$ [26] and Y_2O_3 [27]. $KGdF_4$ with orthorhombic structure has been prepared by solid-state and hydrothermal methods [28,29], while co-precipitation route was applied to assess the influence of fluoride structures and the synthesis method on structural and optical properties of potassium gadolinium fluoride [30]. You et al. prepared orthorhombic $KGdF_4$ phosphors with hydrothermal route and presented the samples with higher quantum cutting efficiency compared to that of $NaGdF_4$ phosphors with Eu^{3+} doping [31]. Moreover, Karbowiak and his coworkers studied the structural and luminescence properties of $KGdF_4$:Eu^{3+} NCs with heat treatment at different temperatures and crystallite sizes [30,32], and they prepared cubic $KGdF_4$:Eu^{3+} NCs and explored their luminescence properties.

---

* Corresponding author. Tel.: +86 020 84113903.
** Corresponding author at: State Key Laboratory of Optoelectronic Materials and Technologies, School of Physics and Engineering, Sun Yatsen University, No. 135, Xingang Xi Road, Guangzhou, Guangdong 510275, PR China.
Tel.: +86 020 84113903.
E-mail addresses: stsyshh@mail.sysu.edu.cn (S.H. Yang), stszyl@mail.sysu.edu.cn (Y.L. Zhang).

0022-2313/$ - see front matter © 2013 Elsevier B.V. All rights reserved.
http://dx.doi.org/10.1016/j.jlumin.2013.04.052

Many efforts have been made to explore the ET mechanism between Gd^{3+} and Eu^{3+} in above-mentioned host lattices. In addition, cubic $KGdF_4$ phosphors doped with Ln^{3+} were studied recently [33–35]. However, there are few studies about the ET process in Eu^{3+}–Eu^{3+} couple and Gd^{3+}–Eu^{3+} couple in $KGdF_4$ host lattice up to now. In this work, we prepare a series of $KGd_{1-x}Eu_xF_4$ nanophosphors with cubic phase and investigate their luminescence properties. We also observe the concentration quenching phenomenon and describe the nonradiative ET mechanisms of the phosphors under different excitation conditions.

2. Experimentation

2.1. Materials

The starting materials are listed as follows: Gd_2O_3 (99.99%, Alladin Reagent Inc. Shanghai, China), Eu_2O_3 (99.9%, Sinopharm Chemical Reagent Co. Ltd. Beijing, China), NH_4HF_2 (AR, Alladin Reagent Inc. Shanghai, China), K_2CO_3 (99%, Guangzhou Chemical Reagent Factory, Guangzhou, China), citric acid monohydrate (99.5%, Richjoint Chemical Reagent Ltd. Shanghai, China) and HNO_3 (65%, Guangzhou Chemical Reagent Factory, Guangzhou, China). All reagents are used without further purification.

2.2. Procedure

$KGd_{1-x}Eu_xF_4$ NCs were prepared by a hydrothermal route in this work. To be specific, 1 mmol Ln_2O_3 (Ln=Gd, Eu) powders were dissolved in HNO_3 while heating with the water-bath method and stirring till excess nitric acid evaporated. 5 mL deionized water was subsequently added with citric acid monohydrate to stir for 10 min to form $Ln(NO_3)_3$ solution. NH_4HF_2 and K_2CO_3 were mixed together with deionized water followed by agitation. Then the mixture was added into the $Ln(NO_3)_3$ solution to form a stable milky suspension and kept stirring for 10 min. At the end, the milky colloid was covered in Teflon, sealed in an autoclave and treated under 200 °C for 12 h before cooling down naturally. The final products were collected by centrifugation, and washed several times with ethanol and then dried at 60 °C overnight.

2.3. Characterization

The phase and structure of the as-prepared nanoparticles were characterized by using a D-Max 2200VPC X-ray diffractometer from Rigaku Company. TEM and high-resolution TEM (HRTEM) were performed on a JEM-2010HR TEM operated at 120 kV from JEOL. The room temperature (RT) photoluminescence (PL) spectra and luminescence lifetime measurements were carried out in an FLSP920 combined fluorescence life and steady-state fluorescence spectrometer equipped with a 450 W xenon lamp and a μF900 pulsed lamp from Edinburgh Instrument Ltd.

3. Results and discussion

3.1. Structure and morphology

The $KGd_{1-x}Eu_xF_4$ NCs present cubic phase from the XRD patterns, as shown in Fig. 1(a)–(i), which does not match the reported orthorhombic $KGdF_4$. Instead, the system shows similarities to α-$NaGdF_4$ (JCPDS No. 27-0697, $a=5.52$ Å, group Fm3m, $Z=2$), with peaks shifting to lower 2θ due to larger cell parameter of $KGdF_4$ compared to $NaGdF_4$ as K^+ replaces Na^+. According to the XRD patterns, the cell constant ($a=5.767$ Å) was determined by using Jade5.0 software, which is close to the reported result [33]. By constructing the unit cell model of $KGdF_4$ based on the cubic fluorite structure through utilizing the Diamond 3.2 software, as shown in Fig. 1, where K^+ and Gd^{3+} randomly replace half of the cation positions and each cation/vacancy is surrounded by eight fluorions [36], the calculated diffraction peaks (represented by star marks shown in Fig. 1) have a good match with those in measured XRD patterns. In addition, no particular difference of full width at half maximum of XRD peaks is observed and according to Scherrer's formula, $D=K\lambda/\beta\cos\theta$, particle sizes of all the samples do not change obviously. The TEM images have revealed that the prepared samples were nano-sized of about 36 nm in average (shown in Fig. 2a and the inset). The lattice fringes can also be observed from HRTEM images (Fig. 2c and d) with an interplanar distance about 2.7 Å of (2 0 0) lattice plane and 3.45 Å of (1 1 1) lattice plane. Finally, we also obtain the electron diffraction pattern of selected areas (Fig. 2b) and mark several major lattice planes calculated from XRD patterns in accordance with the reciprocity relationship.

3.2. Downconversion luminescence performance

3.2.1. Direct excitation of Eu^{3+}–Eu^{3+} couple and sensitized excitation of Gd^{3+}–Eu^{3+} couple

Photoluminescence excitation (PLE) and PL spectra of $KGd_{0.95}Eu_{0.05}F_4$ and $KEuF_4$ NCs are shown in Fig. 3. Sharp peaks around 272.4 nm and 310 nm in $KGd_{0.95}Eu_{0.05}F_4$ represent the energy transitions from ground state $^8S_{7/2}$ to excited states ^6I_J, ^6P_J of Gd^{3+} and those around 393 nm from $^7F_0$ to ^5L_J of Eu^{3+},

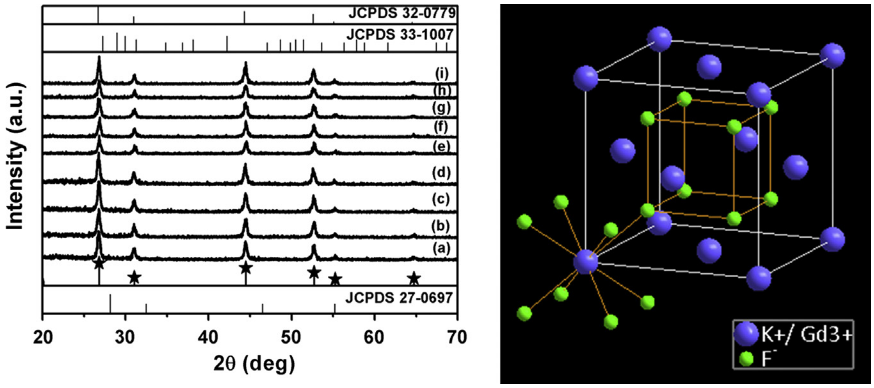

Fig. 1. (Left) XRD patterns of $KGd_{1-x}Eu_xF_4$ NCs. a–i refer to 1, 5, 10, 15, 20, 40, 60, 80 and 100 mol% correspondingly. The stars demonstrate the calculated diffraction peaks of $KGdF_4$ based on the model of $NaGdF_4$. The vertical lines show the standard profiles of JCPDS 27-0697 $NaGdF_4$, JCPDS 33-1007 $KGdF_4$ and JCPDS 32-0779 KEu_2F_7. (Right) Schematic illustration of cubic $KGdF_4$ structure with Diamond 3.2 software. Larger blue circle ● represents (1/2)Gd^{3+} and (1/2)K^+; smaller green circle ● represents F^-. (For interpretation of the references to color in this figure, the reader is referred to the web version of this article.)